

Thermal barrier effect estimation of a new refractory enamel

I. PENCEA, M. MICULESCU*, M. PENCEA^a, C. E. SFAT, M. BRANZEI, V. MANOLIU^b

University "Politehnica" of Bucharest, 202 Splaiul Independentei, 060042, Bucharest, Romania

^a, „Viaceslav Harnaj” High School, Bucharest, Romania

^bNational Institute for Aerospace Research, Bucharest, Romania

New enamel refractory coatings were obtained at National Institute for Aerospace Research, Bucharest, Romania. The enamel was produced to protect the hot working surface of aircraft engines i.e. burning chamber, fire tube, volets etc. The enamels are designed to coat pieces made of super alloys sheets as EI 435, EI 468 etc grades. To assess the thermal barrier effect (TBE) of the two new enamels, named NESA 1 and NESA 2, there were done measurements of thermal diffusivity, scanning electron microscopy (SEM) and X-ray fluorescence spectroscopy (EDP-XRFS). In this respect, the thermal diffusivity and thermal conductivity of coated and uncoated EI 435 samples were measured by Flash method using a FLASHLINE3000 Diffusivity system. The thermal barrier effect of NESA enamels were estimated by two parameters e.g. relative difference of thermal diffusivities and relative difference of time required for the back surface to reach half of the maximum temperature rise. The second parameter seems to be a more confident one from the direct meaning point of view. The SEM investigations were used to assess the morphology of enamel coat and of the interface between enamel and super alloy that is essential for coating TBE and its lifetime. The EDP-XRFS analyses are most fitted to check the correlation among frit, barbotine and fired enamel chemical composition. A XEPOS SPECTRO EDP-XRFS were used for chemical analysis of NESA 1 and NESA 2 samples.

(Received February 06, 2009; accepted May 25, 2009)

Keywords: Enamel, Thermal barrier effect, Thermal diffusivity, SEM investigation, EDP-XRFS analysis

1. Introduction

The metallic surfaces of the turbo reactor engine pieces that come in contact with the hot burned gases are subjected to high temperature (800 – 1150 °C) corrosion and to erosion due to high speed (~ 1 Mach) of solid particles contained in the liquid fuel as pyrolytic carbon, inorganic particles etc.[1,2]. It was proven that the uncoated pieces made of refractory super alloys sheets have a reduced lifetime in the above mentioned work conditions, due to a very severe corrosion caused by Na, V, P, Ca, Fe, Mg etc at temperatures over 800°C even their concentrations in the burned gas are of the ppm orders (1-15ppm)[1]. Thus, the coating of these pieces becomes a must and there are only a few practical solutions in this case: metallization, plasma - spray coating, enamelling. The last solution seems to be the best because it has the highest efficiency-cost ratio. The enamel coatings can increase the work time of the hot working pieces at least two times because they protected the surfaces against the majority damage factors as: erosion, hot corrosion- being impenetrable by hot gas. [1,2]. On the other side, the enamel could protect the superalloy against thermal shock and could play a thermal barrier role between hot gas and metal surfaces. In the above context the goal of the research team was to develop proper enamel coatings for burning camera, fire tube and other pieces made of EI 435 Ni base super alloy. The enamel coatings should be properly characterized to assess their working characteristics as adhesion, thermal shock resistance, TBE and working lifetime [1, 3, and 4]. By SEM, EDP-XRFS and diffusivity tests we tried to achieve as many data as to assess the TBE of the enamel coatings and to find the effective way to improve TBE. The common sense of thermal barrier is the

resistance against temperature increasing but the associated parameter is not well defined. Thus, in this paper we present some considerations on the estimation of thermal barrier by two parameters: relative difference of thermal diffusivities and relative difference of the half time maximum of rear side temperature.

2. Theory

Thermal diffusivity, which can be related to thermal conductivity by multiplying by the product of density and heat capacity per unit mass, is often measured for bulk materials and freestanding coatings by the laser flash technique. ASTM E 1461 addresses the use of flash methods for measurement of bulk materials and could be extended to coated materials. [3, 5]

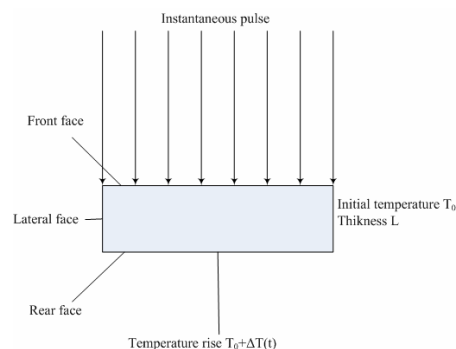


Fig.1. Schematic of the flash method [5].

The laser flash method was used for the estimation of TBE. The schematic representation of flash method is given in Fig 1.

The mathematical expression of the temperature is [6]:

$$T(x,t) = \frac{1}{L} \int_0^L T(x,0) dx + \frac{2}{L} \sum_{n=1}^{\infty} \exp\left(-\frac{n^2 \pi^2 \alpha t}{L^2}\right) \cdot \cos \frac{n\pi x}{L} \int_0^L T(x,0) \cos \frac{n\pi x}{L} dx \quad (1)$$

where α is the thermal diffusivity of the material

At the rear surface, where $x=L$, the dependence of temperature on time has a specific profile as is shown in Fig. 2.

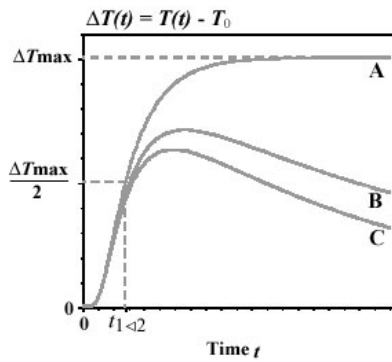


Fig. 2. Characteristic graph of rear temperature evolution in time for the flash method [5].

The mathematical expression of $T(L, t)$ is:

$$T(L,t) = \frac{Q}{\rho \cdot C \cdot g} \left[1 + 2 \sum_{n=1}^{\infty} (-1)^n \cdot \exp\left(-\frac{n^2 \pi^2 \alpha t}{L^2}\right) \right] \quad (2)$$

If one introduces the notations:

$$V(L,t) = \frac{T(L,t)}{T_M} \quad \text{and} \quad \omega = \frac{\pi^2 \alpha t}{L^2} \quad \text{then the expression in}$$

eq.(2) becomes:

$$V = 1 + 2 \sum_{n=1}^{\infty} (-1)^n \exp(-n^2 \omega) \quad (3)$$

when $V = 0.5$ and $\omega = 1.38$:

$$\alpha = \frac{1.38 \cdot L^2}{\pi^2 t_{1/2}} \quad (4)$$

or

$$\alpha = 1.38 \frac{L^2}{t_{1/2}} \quad (5)$$

where: where $t_{1/2}$ is the time required for the back surface to reach half of the maximum temperature rise

On the base of thermal diffusivity one could calculate thermal conductivity if specific mass heat capacity and mass density are known..

The sample undertaken investigations are disks of 12.5mm in diameters. The enamel coated samples NESA 1 and NESA 2 were laser flashed on enamel side while the rear side was uncoated. The reference sample was an uncoated sample i.e. identical with the substrate of enamel of EI 435 superalloy. The exposed surfaces were sprayed with graphite solution and drayed before laser flushed. Thus, we consider the enamel coated samples as similar with the uncoated sample but made of a different material having a greater thickness (with the enamel layer thickness). Thus, we applied the above described mathematical model to the uncoated and enamel coated specimens. From the diffusivity point of view, the thermal barrier effect could be estimated by the difference between thermal diffusivity of uncoated sample (α_{uc}) and thermal diffusivity of enamel coated sample (α_c) or better by relative difference, respectively:

$$TBE_{\alpha} = ((\alpha_{uc} - \alpha_c) / \alpha_{uc}) \cdot 100 (\%) \quad (5)$$

On the other side, the thermal barrier effect could be interpreted as time delaying in reaching a temperature in the case of coated sample versus an uncoated sample. From the view point of the laser flash method we used it is more fitted to consider the thermal barrier as the the difference between $t_{1/2}$ for the uncoated sample and ($t_{1/2uc}$) and $t_{1/2}$ for enamel coated sample ($t_{1/2c}$) or better their relative difference, respective:

$$TBE_{t_{1/2}} = ((t_{1/2uc} - t_{1/2c}) / t_{1/2uc}) \cdot 100 (\%) \quad (6)$$

3. Experimental

The NESA enamel coating is designed to protect burning camera and volets made of EI 435 superalloy sheets (Fig. 3).



(a)



(b)

Fig. 3. Enamel coatings; (a) NESAs enamel on EI 435 substrate(x5); (b) NESAs 2 coaed volet.

The colour of NESAs coating in Fig. 3 differ do two spectral composition not light during picture taken. The elemental composition of EI 435 is given in Table 1.

Table 1. EI 435 elemental compositions.

(%)	W	C	Si	Mn	Al	Ti	Fe	Cr	Ni
EI435	<0.1	0.11	0.72	0.5	0.13	0.27	5.1	4.1	Rest

The elemental composition and thermal expansion coefficient (TEC) of enamel substrate plays a critical role in enamel adhesion and enamel accommodation to substrate. The NESAs enamel with the frite and barbotine composition given in Table 2 and Table 3 has given the best results among the other similar enamels with different compositions.

Table 2. NESAs enamel frite composition.

Oxide s	SiO ₂	BaO	Zn O	ZrO	CaO	Mo ₂ O ₃	MgO	Othe r
%mass	45.0	39.0	5.0	3.0	2.5	2.0	2.5	2.0

Table 3. The NESAs enamel barbotine composition related to frite mass as 100%.

substances	Frite	Cr ₂ O ₃	MT530 argile/clay	Distilled-water	NaO
% mass	100	42.0	10	71	3

The crude enamel was obtained using a classical wet technology including a 96 hours ageing stage and a special percolation graded of the aged barbotine. The EI 435 sheet samples of different sizes, mainly of 100x40±1.2 mm, and representative pieces were prepared for enamel coating by corindon grinding (sand blasting) followed by alcohol washing. The samples were coated by spray technique.

The crude (green) enamel coatings were dried in a clean atmosphere at room temperature for several hours and subsequently, in an electric oven at 120°C for about 2 hours. The dried enamel coated samples had been being fired for about 4 minutes at 1180°C in an electric oven. Finally, enamel coatings of about 0.16 mm in thick were obtained.

The thermal diffusivity of enamel coated specimens and uncoated were estimated from measurements done with an ANTER Corporation FlashLine 3000 Diffusivity system. The tested samples were disks 12.65 mm in diameter and 1.2 mm thickness, coated by sprayed graphite as it is required by this method. Thermal diffusivity (ASTM E1461) and thermal conductivity of the samples were measured from room temperature to 900°C by the Flash Method [6, 7]. The thermal conductivity can be calculated using specific ANTER software by comparing the temperature rise of the sample to the temperature rise of a reference sample of known values tested in the same conditions.

The microstructures and element distributions across the interfaces (X-ray mapping) of the interesting untested and tested samples were investigated with a TEMSCAN C100 X.

The spectrochemical analyses of NESAs enamels were done with a XEPOS SPECTRO ED(P)- XRF spectrometer using Fusion analytical program.

4. Results and discussion

The surface morphologies of enamel coatings were visually evaluated by different optical accessories (see Fig. 1). The characteristic morphologies of NESAs coatings are shown in Fig. 3 (a, b). As resulted from Fig 3 and from many others SEM observations the enamel under consideration has a composite micrometer grained morphology.

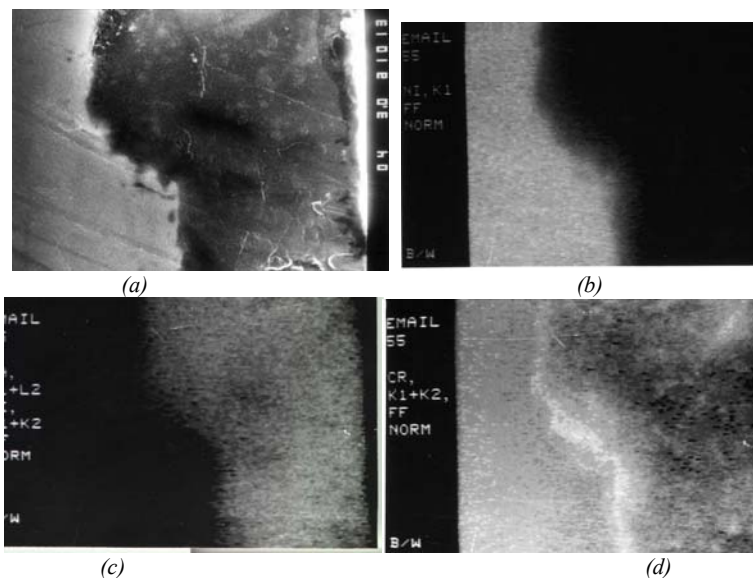


Fig. 3. SEM and EDS images of enamel - EI435 interface: (a) interface SEM image; (b) Ni distribution; (c) Ba distribution; (d) Cr distribution.

The composite morphology creates a net of boundaries which causes discontinuities in spatial distribution of thermal diffusivity. We consider that the grain boundary is less thermal conductive and it explains the greater TBE of these enamel coatings comparing with an homogeneous coating.

The very good adhesion of enamel to EI 435 is related to the Cr[1, 8] diffusion across the enamel-substrate interfaces.(Fig. 4, d) while Ni, Ba etc does not contribute to enamel adhesion.

Thus, the firing stage of enamel technology allows the enamel to umectate, dissolve the substrate oxides and incorporates them into enamel layer. We consider that this is the mechanism that took place at the interface and is reliable of enamel adhesion. An intimate contact between enamel and metal decrease the TBE but is desirable for the enamel standing to thermal shock and functionality. The TBE is somehow visiblebut also in the thermal barrier effect of enamel coating (Fig.3 d).

The NESAs enamel very good adhesion to EI 435 super alloys could be assigned to two mechanisms: mechanical ancoration/hitching and chromium bonding by Cr dendrites which had been growing from substrate into enamel during different heating stages as could be seen in Fig. 3 (d).

The necessary Cr for dendrites growing could be provided by both substrate and enamel. It is expected that after a long heating at an elevated temperature the interface Cr enrichment would achieve a saturation level and it would increase if the heating temperature increases.

The Cr distribution related to Cr_2O_3 and metallic Cr (Fig. 3) shows the most interesting features as Cr inhomogeneous distribution and Cr concentration at the enamel - EI435 interface.

Table 4. Spectrochemical data on NESAs enamel.

Oxide/Element	Z ¹	Element	C ²	Us ³	Units
Na2O	11	Sodium	2,62	0,16	%
MgO	12	Magnesium	2,18	0,08	%
Al2O3	13	Aluminum	1,97	0,05	%
SiO2	14	Silicon	28,22	0,12	%
P2O5	15	Phosphorus	5243	32	ppm
SO3	16	Sulfur	0,5371	0,0089	%
Cl	17	Chlorine	< 2,0	0	ppm
K2O	19	Potassium	0,095	0,003	%
CaO	20	Calcium	4,34	0,09	%
TiO2	22	Titanium	0,411	0,015	%
V2O5	23	Vanadium	< 1,8	0	ppm
Cr2O3	24	Chromium	27,69	0,02	%
MnO	25	Manganese	< 1,3	0	ppm
Fe2O3	26	Iron	0,66	0,09	%
CoO	27	Cobalt	< 3,9	0	ppm
NiO	28	Nickel	0,312	0,006	%
CuO	29	Copper	< 0,6	0	ppm
ZnO	30	Zinc	2,12	0,01	ppm
Ga	31	Gallium	< 0,5	0	ppm
Ge	32	Germanium	0,5	0	ppm
Se	34	Selenium	< 0,5	0	ppm
Br	35	Bromine	< 0,3	-0,2	ppm
Rb2O	37	Rubidium	4,8	0,2	ppm
SrO	38	Strontium	1760	2	ppm
YO3	39	Yttrium	6,9	0,3	ppm

Table 4 (continuation)

Oxide/Element	Z ¹	Element	C ²	U _s ³	Units
ZrO ₂	40	Zirconium	1.74	0,05	%
Nb ₂ O ₅	41	Niobium	< 1.4	0	ppm
Mo ₂ O ₃	42	Molybdenum	2.31	0.09	%
Ag	47	Silver	< 2.0	0	ppm
Cd	48	Cadmium	< 2.0	0	ppm
SnO ₂	50	Tin	< 3.9	0	ppm
Sb ₂ O ₅	51	Antimony	< 4.0	0	ppm
Te	52	Tellurium	< 3.0	0	ppm
I	53	Iodine	< 3.0	0	ppm
Cs	55	Cesium	< 4.0	0	ppm
BaO	56	Barium	24.62	0.07	%
La	57	Lanthanum	< 2.0	0	ppm
Ce	58	Cerium	< 2,0	0	ppm
Hf	72	Hafnium	144.4	3.2	ppm
Ta ₂ O ₅	73	Tantalum	1780	21	ppm
WO ₃	74	Tungsten	1071	18	ppm
Hg	80	Mercury	< 0.0001	0	%
Ta	81	Thallium	< 0.0001	0	%
PbO	82	Lead	54.1	1.1	ppm
Bi	83	Bismuth	< 1.0	0	ppm
Th	90	Thorium	< 1.0	0	ppm
U	92	Uranium	15.9	0.5	ppm

Z¹-atomic number; 2-C-concentration; 3-U_s-standard uncertainty

The spectrochemical compositions of NESA are given in Table 4. As it can be seen the enamel coat has a very

complex oxides composition that could be assigned to the raw materials in barbotine composition. To our knowledge, is for the first time when enamel composition is quantified including standard uncertainty. There were some previously attempts to estimate the enamel composition by XRFS but only at qualitative level [2]

Spectrochemical composition of NESA is close to the expected one for the main oxides but reveals the presence of other oxides as Al₂O₃, NiO, Fe₂O₃ and PbO. These oxides could come from MTS clay or from other sources that interfere with the enamel preparation process. The critical elements as Cd, Hg, Bi are below the quantification limits while others as SrO and U are quite at the limit of detection of the spectrometer.

SEM and EDP-XRFS data show that the enamel coatings are of oxides nature, with a micro composite compact structure. The enamel coatings have very good adhesions to super alloy substrates and the enamel-substrate interfaces have rough morphology with average thickness of about 20 μm. These aspects depict a two layer structure of the sample with a quasi-continuous transition from enamel to the substrate e.g. it could be considered that thermal expansion coefficients and, more important, thermal diffusivity coefficients suffer a continuously transition from enamel to substrate. These aspects explain the proper working of enamel coatings at elevated temperature and their resistance to thermal shock [1, 9]. Based on above facts we considered the enamel coated sample as a continuous solid body of disk shape. When such a sample is laser flashed a heat flux pass smoothly i.e. as a smooth function of sample thickness. In this sense, our samples comply Taylor's theory criteria for the diffusivity measurement using flash method.

The thermal conductivity of the sample could be calculated for the coated sample and the uncoated sample using the Anter analysis software. The results of thermal diffusivity and thermal conductivity are given in the Table 5 and Table 6. The sample shape and the coating thickness ensure insignificant radial heat losses and a good accuracy of the measurements. There were flashed two NESA enamel coated samples one of 0.09 mm in thickness and other of 0.17 mm, called NESA 1 and NESA 2, respectively. The uncoated sample is named EI-435.

Table 5. Mean thermal diffusivity.

Nr Crt.	NESA 1		NESA 2		EI 435	
	Temp.	cm ² /s × 10 ⁻³	Temp.	cm ² /s × 10 ⁻³	Temperature	cm ² /s × 10 ⁻³
1	116	35.6	116	32.5	113	37.7
2	216	37.9	216	34.2	214	39.3
3	314	40.3	314	35.9	312	42.0
4	412	42.5	412	37.3	409	44.4
5	510	44.2	510	38.2	508	46.5
6	608	46.1	609	39.3	608	49.2
7	707	47.7	709	39.8	703	50.2
8	807	48.4	808	41.1	801	52.3
9	908	49.0	910	42.3	900	53.0

Thermal diffusivities of NESAs 1, NESAs 2 and EI 435 samples (Fig. 4) increase slightly with temperature. The difference among diffusivities increases with temperature. Thermal diffusivity of NESAs 2 is the smallest and less dependent on temperature in the range 100 - 900 °C.

Thermal conductivity of NESAs 1, NESAs 2 samples (Fig. 5) increases slightly with temperature while of EI 435 sample increases strongly in the range 650-850°C (Fig. 5).

Table 6. Mean thermal conductivity.

Nr Crt.	NESAs 1		NESAs 2		EI 435	
	Temperature	W/mK	Temperature	W/mK	Temperature	W/mK
1	116	10.3	116	13.6	113	10.1
2	216	11.9	216	14.3	214	11.8
3	314	13.4	314	15.3	312	13.9
4	412	14.4	412	16.1	409	15.0
5	510	15.4	510	16.5	508	16.3
6	608	16.2	609	16.8	608	18.0
7	707	17.4	709	17.7	703	35.7
8	807	17.6	808	18.1	801	40.2
9	908	17.8	910	18.3	900	42.3

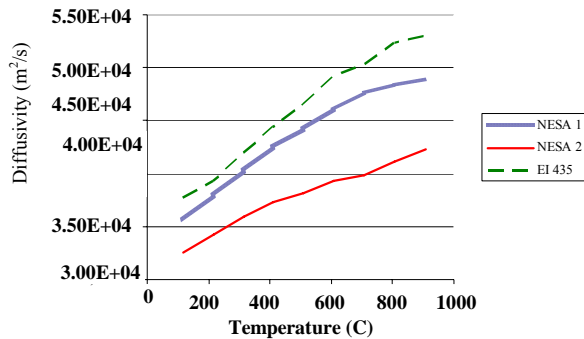


Fig. 4. Thermal diffusivity variation with temperature.

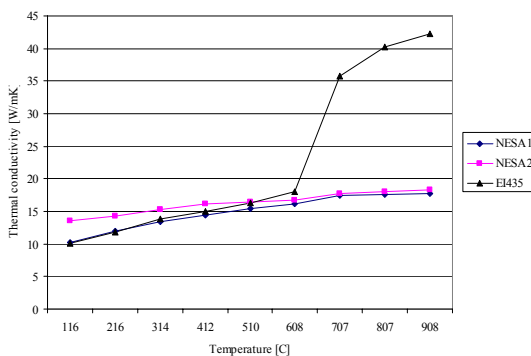


Fig. 5. Conductivity variation with temperature for the tested samples.

The TBE of sample NESAs 1 and NESAs 2 estimated on the base of rel.(5) and rel. (6) are given in Table 7.

Table 7. TBE_{α} and $TBE_{1/2}$ for NESAs 1 and NESAs 2 samples.

Nr crt.	Temp.	$(\alpha_{EI435} - \alpha_{NESAs1}) / \alpha_{EI435}$	$(dt_{NESAs1} - dt_{EI435}) / dt_{EI435} * 10^0$	$(\alpha_{EI435} - \alpha_{NESAs2}) / \alpha_{EI435}$	$(dt_{NESAs2} - dt_{EI435}) / dt_{EI435} * 10^0$	
1	116	6	6	14	16	13
2	216	4	4	13	15	14
3	314	4	4	15	17	13
4	412	4	4	16	19	17
5	510	5	5	18	22	20
6	608	6	7	20	25	22
7	707	5	5	21	26	21
8	807	7	8	21	27	25
9	908	8	8	20	25	22

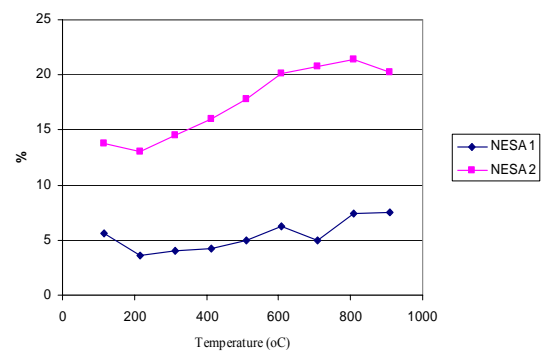


Fig. 6. Relative difference of thermal diffusivities.

The TBE_{α} of the sample NESAs 1 and NESAs 2 at different temperature are given in Fig. 6. From Fig. 6 it results clear that NESAs 2 has the best TBE and is around 20% at working temperature. The thickness is greater as the TBS increases.

From the $TBE_{1/2r}$ point of view, the TBE of the enamel coated sample NESAs 1 and 2 is greater (Fig. 7) and is around of 26% at elevate temperature for NESAs 1 and 2. The same, the $TBE_{1/2r}$ of the sample NESAs 1 is about 50% of NESAs 2 as in the previous estimation by TBE_{α} .

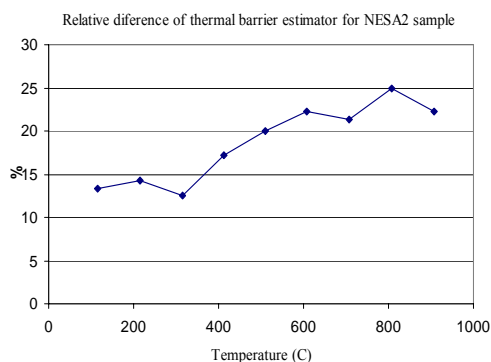


Fig. 7. Temperature dependence of $TBE_{1/2r}$ for sample NESAs 2.

5. Conclusions

The TBE of NESAs enamel coatings were estimated by two parameters: the relative difference of thermal diffusivity (TBE_{α}) and relative difference of the time required for the back surface to reach half of the maximum temperature rise ($TBE_{1/2}$).

From the effectiveness point of view, $TBE_{1/2}$ seems to be more adequate for TBE quantification than TBE_{α} .

The enamel NESAs 2 increases the TBE of coated sample with about 25% related to uncoated one at elevate working temperatures (750–850 °C).

The enamel coating TBE is quite proportional with their thickness in the range of 0.1–0.2 mm.

The interface morphology and elemental distributions (Fig. 3) show that enamel coating adheres well to substrate and, more important, ensures a smooth transition of diffusivity gradient.

ED(P)XRF and SEM-EDS cooperative investigations on enamel coating provide valuable data that contribute to a better understanding of TBE and to a further improving of enamel coating adhesion and TBE.

The researches presented in this paper will be continued for a more fundamental theoretically assessing of enamel TBE and for a more accurate TBE measurement including uncertainty estimation of TBE according SR EN ISO 13005:2005, EA 016 and other in force regulations.

- [1] C. Dumitrescu, I. Pencea, D. Bunea, V. Manoliu, F. Vasiliu, F. Barca, R. Paunescu, 1999, 1st Int. Conf. The Coatings Proc. Thessaloniki-Greece, 303.
- [2] G. Carlanescu, C. Puscasu, M. Grigorescu, N. Constantin, *Metalurgia International* **XIII**(3), special issue 63, 2003.
- [3] S. J. Dapkuna, *J. of Thermal Spray Technology* **6**(1), 67 (1997).
- [4] Y. Xiong, C. Guan, S. Zhu, F. Wang, *J. Mater. Eng. Perform.* **15**(5), 564 (2006).
- [5] W. J. Parker, R. J. Jenkins, C. P. Butler, G. L. Abbott, *J. Appl. Phys.* **32**, 1679 (1961).
- [6] L. Vozár, 2001 Flash Method for the Thermal Diffusivity Measurement, Theory and Praxis (Nitra, UKF).
- [7] I. Pencea, F. Vasiliu, M. Britchi, M. Olteanu, *Int. J. of Materials & Product Technology* **6**(6/7), 658.
- [8] H. J. Lee, *Thermal Diffusivity in Layered and Dispersed Composites* Thesis Purdue University Lafayette Ind., 1975.
- [9] H. J. Lee, R. E. Taylor, *Determination of Thermophysical Properties of Layered Composites in Thermal Conductivity 14*, New York, Plenum Press, 423, 1976.
- [10] J. N. Sweet, *Effect of Experimental Variables on Flash Thermal Diffusivity Analysis in Thermal Conductivity 20* New York, London, Plenum, 287, 1989.
- [11] W. Hohenauer, L. Vozár, *Estimation of Thermophysical Properties of Layered Materials Using the Laser Flash Method High Temp. – High Press.* **33**, 17, 2001.

*Corresponding author: marian@sim.pub.ro